International Journal on Robotics, Automation and Sciences

Fuzzy Frontiers in Rift Valley Fever Virus Control: Exploring the Dynamics of Transmission and Treatment

Meyyappan Sangavi, M. Vidhya Lakshmi, Murugappan Mullai*, Grienggrai Rajchakit* and Govindan Vetrivel

Abstract **- Rift Valley Fever (RVF) is a mosquito-borne zoonotic viral disease that poses significant health threats to both human and animal populations across Africa and parts of the Middle East. Traditional epidemiological models often assume precise parameter values, which may not accurately reflect the inherent uncertainty in real-world disease transmission. To address this, we propose a novel stochastic and fuzzy logic-based Susceptible-Infected-Susceptible (SIS) model to analyze the spread of RVF under uncertain conditions. The model incorporates fuzziness in transmission and recovery rates using fuzzy set theory. Equilibrium points are analytically derived, and stability analysis is performed to explore the long-term dynamics of the disease. We compute and compare the fuzzy expectation of infected individuals with the classical expectation to assess the effect of parameter uncertainty. The basic reproduction number R_0 is calculated for both strictly increasing and strictly decreasing transmission functions, and their impacts on transcritical and backward bifurcations are thoroughly investigated. Furthermore, we incorporate optimal control strategies, including vaccination and vector control, within the fuzzy framework and evaluate how uncertainty influences their effectiveness. Numerical simulations validate the analytical results and illustrate the temporal progression of the disease. Our findings emphasize that integrating fuzzy logic with stochastic modeling provides a more realistic and robust approach to understanding and controlling RVF than conventional deterministic models, offering valuable insights for public health intervention planning under uncertainty.**

Keywords—Rift Valley Fever, Fuzzy SIS model, Equilibria, Stability, Numerical Simulation.

I. INTRODUCTION

Contemporary global health faces an escalating burden from infectious pathologies, which now demand urgent scholarly and political attention. These morbid entities bear profound responsibility for the rising incidence of physiological impairments and mortality within Homo sapiens populations. The confluence of climatic perturbations, intensified global mobility, and antimicrobial resistance has precipitated recurrent epidemics of virulent pathogens including H1N1 influenza, Zika virus, and hemorrhagic fevers. use another word for pathogen mortality incidence [18,40,1,15,16,36,19,9]. Murray [29] expounded upon various theoretical aspects of epidemiology in his

*Corresponding Author email: mullaim@alagappauniversity.ac.in, ORCID: 0000-0001-5762-1308; kreangkri@mju.ac.th, ORCID: 0000-0001-6053-6219.
Meyyappan Sangavi, Department of Mathematics, Alagappa University, Karaikudi, Tamilnadu, India. (email: sangavispark@gmail.com)
M.Vidhya Lakshmi, Department of Mathematics, Alagappa University, Karaikudi, Tamilnadu, India. (email: vidhyamaran17@gmail.com)
Murugappan Mullai* working as an Assistant Professor (CDOE) of Mathematics, Alagappa University, Karaikudi, Tamilnadu, India. Also, she is a research fellow of INTI International University, Nilai Campus, Malaysia.
Grienggrai Rajchakit*, Associate Professor, Department of Mathematics, Faculty of Science, Maejo University, Chiang Mai 50290, Thailand.
Govindan Vetrivel, Department of Mathematics, Alagappa University, Karaikudi, Tamilnadu, India. (email:menakagovindan@gmail.com)

International Journal on Robotics, Automation and Sciences (2025) 7, 2:8-21
https://doi.org/10.33093/ijoras.2025.7.2.2
Manuscript received:8 Apr 2025 | Revised: 31 May 2025 | Accepted: 19 Jun 2025 | Published: 30 Jul 2025

Published by MMU PRESS. URL: http://journals.mmupress.com/ijoras

seminal work. The pioneering efforts in quantitative analysis of disease spread can be attributed to Kermack and McKendrick [6], who first conceptualized the simplistic yet foundational SIR model. Since their groundbreaking contribution, theoretical epidemiology has undergone substantial evolution, witnessing the introduction of myriad refinements and sophisticated methodologies. Diverse strategies have been integrated into epidemic models to mitigate disease spread. Among these, immunization, medical intervention, quarantine[17], and insecticide application [16] stand as prominent control measures actively employed within society. Numerous scholars have extensively explored immunization as a containment strategy, including Arino et al. [4], Makinde [24], Jana et al. [16], and Thomasey and Martcheva [34]. Conversely, therapeutic approaches have been examined by scientists, such as Gunel and Moghadas [12], Qiu and Feng [25], Hu et al. [14], and Zhou and Fan [41]. A subset of studies, including those by Kar and Jana [18,16], Brauer [7], Okosun et al. [30], and Laarabi et al. [22], has delved into the combined efficacy of both immunization and therapeutic interventions. The propagation patterns of infectious diseases are governed by various parameters that dictate the pace at which an infected individual transmits the disease to vulnerable hosts. Classical epidemic models, as outlined by Hethcote [13], predominantly incorporate bilinear and standard incidence levels. In 1973, Capasso and Serio [8] gave a saturating incidence function $g(I)S$, wherein $g(I)$ asymptotically approaches a saturation threshold as the affected group expands. Mathematically, this is expressed as $g(I) = \frac{kI}{1+\alpha I}$, where kI denotes the infectious force, while $\frac{I}{1+\alpha I}$ encapsulates the inhibitory influence stemming from behavioral adaptations of vulnerable individuals or the crowding effect of contagious individuals. Further advancements in modeling incidence functions were made by Ruan et al. [32], who analyzed epidemic dynamics under nonlinear incidence functions. A general incidence function $g(I)S = \frac{KI^pS}{1+\alpha I^q}$, where $p > 0, q > 0$, was provided by Liu et al. [37] and by numerous other research people. Notably, in the majority of epidemiological studies, the disease transmission function is predominantly assumed to exhibit a linear dependence on the at-risk population. However, owing to the aforementioned factors—such as the inhibitory effect or the heightened vigilance among the at-risk demographic—the infection propagation rate does not invariably adhere to a linear dependency on S. Consequently, we conceptualize it as an arbitrary formulation of S. Furthermore, given the interdependence between the susceptible cohort and the afflicted populace, the disease dissemination dynamics fluctuate accordingly. Thus, we define the transmission coefficient as the product of a linear dependency on the infected populace (I) and an arbitrary functional representation of the susceptible demographic (S). In scenarios where the count of individuals recuperating due to the efficacious execution of treatment protocols is considered, it is conventionally modeled as a linear dependency on the administered therapeutic intervention [1]. Nevertheless, Eckalbar and Eckalbar [10] as well as Zhang and Liu [40] employed a nonlinear therapeutic response function. In a contemporary study, Zhou et al. [42] devised an SIR model incorporating immunization strategies under constrained resource availability. In modern epidemiological modeling, the treatment response function is commonly understood to vary with both the infected cohort (I) and.the therapeutic modulation parameter (u). For the sake of generalization, we define the mitigation-driven therapeutic function exclusively as a flexible formulation in terms of the regulatory parameter (u). Given that both the infection virulence distribution function and the therapeutic response function are selected in an discretionary manner, our study employs the most rudimentary compartmental framework, namely the SIS model, as the basis for our analysis.

Rift Valley fever (RVF) is a viral ailment impacting both anthropoid and ruminant species, manifesting in a spectrum of clinical severities from mild to life-threatening. Mild manifestations include fever, myalgia, and cephalalgia, whereas severe complications may result in ocular impairment or encephalitic infections. The causative agent, the RVF virus, propagates through direct exposure to contaminated animal blood, inhalation of infected aerosolized particles, ingestion of unpasteurized dairy products, or bites from pathogen-carrying mosquitoes, predominantly afflicting bovines, ovines, caprines, and camelids. Interhuman transmission appears improbable. Diagnostic evaluation involves the identification of viral antigens or corresponding antibodies in the bloodstream. Mitigation strategies encompass prophylactic livestock immunization prior to epidemic onset, restriction of animal transit, and vector population suppression. While a human vaccine exists, its availability remains limited, and medical intervention is primarily symptomatic and supportive. RVF epizootics and epidemics predominantly transpire in African and Arabian regions, typically triggered by excessive precipitation, which escalatesmosquito proliferation. Initially documented in Kenya during the early 20th century, the virus was successfully isolated in 1931 amidst an ovine epidemic. The incubation duration spans 2 to 6 days, with the majority of human cases exhibiting either asymptomatic profiles or mild, influenza-like syndromes.

Fuzzy set theory, pioneered by Zadeh [44], provides a robust approach for integrating this uncertainty. Massad et al. [25] previous studies have employed fuzzy logic in epidemic modeling(FEM); notably, Mishra et al. [26] developed a FEM to capture worm transfer patterns in tech box networks, drawing an analogy to the dissemination of infectious diseases. Recent advancements in fuzzy epidemic modeling have sought to capture uncertainties in disease dynamics, but several limitations remain unaddressed. Subramanian et al. (2024)[35] developed a fuzzy fractional SIR model using Caputo

derivatives to account for memory effects in childhood diseases; however, their model did not consider vector-borne transmission or treatment mechanisms. Arif et al. (2024)[3] proposed a hybrid SIR-fuzzy model with numerical simulations to handle uncertain parameters, yet the model assumes a constant population and excludes reinfection, making it unsuitable for SIS-type diseases. Rashidian et al. (2024)[32] focused on exposure risk assessment using fuzzy logic within digital contact tracing frameworks, though their work does not address disease progression or therapeutic interventions. In another study, Arif et al. (2024)[2] constructed a fuzzy HIV/AIDS model with a nonlinear saturated incidence rate, but it is disease-specific and lacks generalizability to vector-borne infections like RVF. Kumar and Susan (2024)[21] introduced a hybrid time-varying SIRD model combined with particle swarm optimization and deep learning to predict epidemic waves; however, they did not incorporate fuzzy logic or uncertainty modeling, which is central to realistic disease forecasting. Mpeshe (2022)[28] formulated a fuzzy SEIR model for amoebiasis that includes environmental considerations, but the model is not designed for mosquito-borne diseases or treatment dynamics. Finally, Azerigyik et al. (2025)[5] reviewed the temperature-dependent dynamics of RVF virus infection in mosquitoes, providing valuable insight into climate impacts but lacking a mathematical modeling framework. In contrast, our study formulates a fuzzy SIS model specifically tailored to Rift Valley Fever, integrating nonlinear incidence and treatment functions with flexible fuzzy parameters. This allows the model to more accurately reflect real-world uncertainty, reinfection dynamics, and intervention responses in the context of a vector-borne disease, filling a critical gap in existing literature. Liu et al. (2023)[23] developed a fuzzy SEIRS model with stochastic noise to study COVID-19 transmission, including quarantine and vaccination, but did not consider vector-borne diseases or nonlinear treatment. Zhou and Wang (2022)[43] proposed a fuzzy fractional-order malaria model using Atangana-Baleanu derivatives to capture memory effects in vector-host dynamics; however, their model assumes perfect treatment efficacy and lacks reinfection or fuzzy control policies. Singh et al. (2021)[34] introduced a fuzzy SEIR model with delay differential equations for dengue transmission, incorporating human movement and environmental factors, yet their model excludes treatment control and vector infection stages. Kumar and Chandra (2020)[20] presented a fuzzy multi-group epidemic model for tuberculosis with age-structured populations, which addresses transmission uncertainty but omits vector-borne dynamics and treatment saturation. Fernandes et al. (2020)[11] applied fuzzy logic to Zika virus transmission modeling by including climate-driven mosquito population dynamics, but did not incorporate nonlinear treatment functions or fuzzy control interventions. These studies highlight ongoing efforts in fuzzy epidemic modeling while underscoring the need for models like ours that integrate nonlinear incidence, treatment, and fuzzy parameters in vector-borne disease contexts.

While classical SIS models and their extensions have been extensively applied to model infectious disease dynamics under deterministic or stochastic frameworks, they often assume that epidemiological parameters are precisely known. However, real-world data—particularly in the context of emerging and neglected diseases such as Rift Valley Fever (RVF)—are fraught with imprecision due to environmental variability, incomplete reporting, and diagnostic limitations. Although a few studies have incorporated fuzzy logic into epidemic models, they typically address generic diseases or theoretical constructs without focusing on region-specific vector-borne zoonotic infections like RVF. The novelty of this study lies in the formulation of a fuzzy SIS model that incorporates uncertain transmission and recovery rates as fuzzy parameters tailored specifically to RVF epidemiology. Unlike previous models, our approach integrates realistic fuzzy membership functions to represent the imprecision in disease spread and recovery dynamics. Additionally, we define general nonlinear forms for transmission and therapeutic functions within a fuzzy framework, enhancing the adaptability and predictive capacity of the model. This allows for a more robust and flexible understanding of RVF dynamics, offering actionable insights for public health planning and targeted intervention strategies under uncertainty. The proposed approach yields more compelling results by accounting for uncertainty and nonlinearity in a modular, computationally feasible framework. This makes it particularly suited for modeling vector-borne diseases like RVF, where precise data is often unavailable and control strategies are environment-dependent.

II. DEVELOPMENT OF THE MODEL

The fuzzy SIS model structurally differs from classical SIS models by incorporating **fuzzy logic-based membership functions** to represent **uncertainty in key epidemiological parameters**—such as transmission rates and recovery rates—which are often assumed to be precisely known in traditional models. In particular, this approach replaces crisp parameters with fuzzy-valued functions that capture **gradual transitions and imprecise thresholds**, such as viral load-dependent transmission or recovery effectiveness. This allows the model to better reflect real-world variability and expert knowledge in uncertain environments where exact data may be lacking or ambiguous. Furthermore, the model structure includes **fuzzy rules and inference systems**, which fundamentally alter the system's dynamics compared to deterministic or purely stochastic counterparts. We rigorously evaluate a standard epidemiological model that classifies the population into 2 compartments: (i) the suspect cohort $S(t)$ and (ii) the infect cohort $I(t)$, both explicitly time-hinged upon. We presuppose that all Agents are introduced into the system as susceptible, and the total population remains conserved—a condition

contingent upon the equivalence of the hiring rate μ and the rate of death μ at any instant t.

Furthermore, we postulate that the pathogen disseminates via direct transmission among the non-infected subpopulation. The incidence rate at which susceptibles acquire infection is denoted by the continuously differentiable function $f(S)$, while therapeutic modulation is governed by the treatment control function $\varphi(u)$, likewise smooth in its argument u. Crucially, we assume immunity is non-permanent; thus, recovered individuals revert to the susceptible state. The resulting dynamical system is formulated as follows:

$$\left.\begin{aligned}\frac{dS}{dt} &= \mu - f(S)I + \phi(u)I - \mu S \\ \frac{dI}{dt} &= f(S) - \phi(u)I - \mu I\end{aligned}\right\} \quad (1)$$

with init. condns.,

$$S(0) \geq 0, \quad I(0) \geq 0 \quad (2)$$

(2)

In this paradigm where population states are characterized by normalized dimensionless measures given by:

$$S(t) + I(t) = 1 \quad (3)$$

The mapping $f: \mathbb{R}_{\geq 0} \to \mathbb{R}_{\geq 0}$ is postulated to be differentiable, continuous and bijective, with the operator $\varphi: \mathbb{R}_{\geq 0} \to \mathbb{R}_{\geq 0}$ satisfying identical regularity conditions.

III.MODEL ASSUMPTIONS AND FUZZY MEMBERSHIP FUNCTION

The fuzzy SIS model is built upon the following core assumptions and corresponding fuzzy membership structures:

The transmission function f (S, v) and the treatment function $\phi(u, v)$ are described using triangular membership functions based on the viral load v\nu. These functions represent the degree of belief regarding low, moderate, and high levels of transmission or treatment effectiveness.

The viral load v\nu within the host population is considered uncertain and not precisely measurable. This uncertainty is modeled using fuzzy sets for low, moderate, and high levels of viral load, denoted by $\mu_L(v)$, $\mu_M(v)$, $and\ \mu_H(v)$ respectively. Each of these fuzzy sets is defined using triangular membership functions, and the key parameters such as the minimum infectious threshold (v_{min}), peak infectivity (v_M), and saturation level (v_{max}) are chosen based on biological or clinical considerations.

The treatment control function $\phi(u, v)$ incorporates uncertainty by being fuzzified to reflect variations in treatment efficacy due to differences in patient responses or drug resistance. It is guided by fuzzy rules, for instance: if the viral load is high, the treatment effect is low; and if the viral load is moderate, the treatment effect is moderate.

A fuzzy inference system is used to apply a rule-based logic that determines the system's behaviour under uncertain inputs. The defuzzified result of this system influences how the model evolves over time in terms of the different epidemiological compartments.

The parameters used in this study are not taken from actual epidemiological data but are selected from biologically plausible ranges to illustrate the qualitative behaviour of the fuzzy SIS model. This approach allows an exploration of structural dynamics, bifurcation behaviour, and potential control strategies in the presence of uncertainty, especially in contexts where clinical data may be limited or unavailable.

To reflect general epidemic patterns and explore how sensitive the model is to different parameter values, these parameters are randomly varied within reasonable intervals. While these values are not empirical, they serve to demonstrate the theoretical potential of fuzzy modelling in uncertain or data-scarce settings.

In this context, generalized functions and fuzzy logic-based extensions are conceptually different. Generalized functions, also known as distributions, are mathematical tools that extend the concept of traditional functions to handle cases involving discontinuities or singularities, such as the Dirac delta function. These are often used in differential equations and integral transforms. On the other hand, fuzzy logic-based extensions introduce uncertainty directly into the model's functions using fuzzy sets and linguistic rules. These methods address epistemic uncertainty in parameters and system behaviour by assigning degrees of membership to values like viral load or treatment efficacy and using fuzzy inference to govern the model's dynamics.

While both approaches generalize classical modeling, they differ in purpose: generalized functions extend analytical solvability, whereas fuzzy logic extends interpretability under imprecision. Our work strictly focuses on the latter—introducing fuzzy membership functions to account for vague thresholds and nonlinear behavior in epidemiological dynamics.

IV.LIMIT STATES AND CONVERGENCE CRITERIA

This segment endeavors to systematically derive all feasible equilibrium states of the system, subsequently examining their stability properties through rigorous analysis predicated upon the fundamental reproduction number (R_0)

Theorem 3.1 *The system (1) admits two biologically meaningful equilibria: a trivial Disease Free Equilibrium (DFE) at (0,1) and a non-trivial Endemic Equilibrium (EE) represented by* (S^*, I^*)*, where*

$$S^* = f^{-1}(\varphi(u) + \mu), I^* = 1 - f^{-1}(\varphi(u) + \mu).$$

Alternatively, these can be rewritten as

$$S^* = f^{-1}\left(\frac{f(1)}{R_1}\right), I^* = 1 - f^{-1}\left(\frac{f(1)}{R_1}\right), \quad (4)$$

where $f(1)$ signifies the pathogen's transmissibility metric evaluated under disease-free conditions. The reprod. no. is given by

$$R_1 = \frac{f(1)}{\varphi(u)+\mu} \quad (5)$$

The EE arises whenever $R_1 > 1$, provided that the disease transmission fn.(DTF) $f(S)$ is strictly increasing with respect to S.

Proof. We can have the equi. Pts. using

$$\frac{dS}{dt} = 0 \quad \text{and} \ \frac{dI}{dt} = 0 \tag{6}$$

Then, we have DFE (1,0) and EE (S^*, I^*) where,

$$S^* = f^{-1}(\phi(u) + \mu)$$

and

$$I^* = 1 - f^{-1}(\phi(u) + \mu)$$

i.e. $S^* = f^{-1}(\frac{f(S^*)}{R_1})$ and $I^* = 1 - f^{-1}(\frac{f(S^*)}{R_1})$ (7)

where, $R_1 = \frac{f(S^*)}{\phi(u)+\mu}$. (8)

The EE exists, when $R_1 > 1$

Stability properties at both trivial and non-trivial equilibria are characterized under the structural assumption that the DTF f(S) is strictly monotonically rising in the susceptible population S.

Theorem 3.2 *While the DTF f(S) is strictly rising, the DFE (1,0) is stable while* $R_1 < 1$ *and unstable for* $R_1 > 1$, *where* $R_1 = \frac{f(1)}{\phi(u)+\mu}$.

Proof. The Jacobian matrix(JM) of (0.1) is

$$J = \begin{pmatrix} -f'(S)I - \mu & -f(S) + \phi(u) \\ f'(S)I & f(S) - \phi(u) - \mu \end{pmatrix} \tag{9}$$

To find the stability at the DFE point, we solve J at(1,0) is

$$J = \begin{pmatrix} -\mu & -f(1) + \phi(u) \\ 0 & f(1) - \phi(u) - \mu \end{pmatrix} \tag{10}$$

The eigenvalues are

$$\lambda_1 = -\mu \quad \text{and} \lambda_2 = f(1) - \phi(u) - \mu. \tag{11}$$

Since λ_1 is negative, stability depends on λ_2. The DFE is asymptot. stable if $R_1 < 1$ (i.e., $\lambda_2 < 0$) and unstable if $R_1 > 1$ (as $\det J < 0$).

Theorem 3.3 *The DFE is globally asymptotically stable if* $R_1 < 1$, *provided* $f(S)$ *is strictly increasing.*

Proof. From the 2nd eqn. of (0.1) we can have

$$\frac{dI}{dt} \leq \big(f(S) - f(1)\big)I \tag{12}$$

As, $f(S) - f(1) < 0$,if $R_1 < 1$,which implies $I(t) \to 0$ as t → ∞.Therefore ,S(t)+I(t) = 1 gives $S(t) \to 1$.

Theorem 3.4 *The EE is asymptotically stable if* $R_1 > 1$, *given that* $f(S)$ *is strictly increasing.*

Proof. The JM at the EE $(S^*, I^*)$is

$$J = \begin{pmatrix} -f'(S^*)I^* - \mu & -\mu \\ f'(S^*)I^* & 0 \end{pmatrix} \tag{13}$$

The trace and det. of the JM J are

$$\mathrm{Tr}(J) = -f'(S^*)I^* - \mu, \mathrm{Det}(J) = \mu f'(S^*)I^*,$$

respectively. Given that $f(S)$ is strictly monotonically increasing, it follows that

$$\mathrm{Tr}(J) < 0, \mathrm{Det}(J) > 0,$$

ensuring local asymptotic stability. The EE is biologically feasible and remains stable if and only if the reproduction threshold satisfies

$$R_1 > 1.$$

Theorem 3.5 *If* $f(S)$ *is strictly decreasing, system (1) has a DFE at* $(1,0)$ *and a unique EE* (S^{**}, I^{**}) *that exists only if* $R_0 < 1$. *The equilibrium values become*

$$S^{**} = f^{-1}\left(\frac{f(S^{**})}{R_0}\right), I^{**} = 1 - S^{**},$$

where the basic reprod. no. is defined as

$$R_0 = \frac{f(S^{**})}{\varphi(u)+\mu}. \tag{14}$$

Proof. We can get the equilibrium point using

$$\frac{dS}{dt} = 0 \text{ and } \frac{dI}{dt} = 0$$

Also, we can have, the DFE (1,0) and EE (S^{**}, I^{**}) where, $S^{**} = f^{-1}(\phi(u) + \mu)$ and $I^{**} = 1 - f^{-1}(\phi(u) + \mu)$ i.e. $S^{**} = f^{-1}(\frac{f(S^{**})}{R_0})$,

$$I^{**} = 1 - f^{-1}(\tfrac{f(S^{**})}{R_0}) \text{ where } R_0 = \tfrac{f(S^{**})}{\phi(u)+\mu}. \tag{15}$$

The EE exists when $R_1 < 1$

With f strictly decreasing, $R_0 > R_1$, so the EE exists if $R_0 < 1$. By Theorem 3, the following result holds.

Theorem 3.6 *A strictly decreasing f(S) ensures that the DFE is stable and unstable when* $R_0 < 1$ *and* $R_0 > 1$.

Theorem 3.7 *For a strictly decreasing transmission function (f'(S) < 0,* $\forall S \in (0, S_0)$*), the EE point is unstable.*

Proof. The JM at the EE $(S^{**}, I^{**})$is

$$J = \begin{pmatrix} -f'(S^{**})I^{**} - \mu & -\mu \\ f'(S^{**})I^{**} & 0 \end{pmatrix} \tag{16}$$

Here, $Tr(J) = -f'(S^{**})I^{**} - \mu$ and $Det(J) = \mu f'(S^{**})I^{**} < 0$.As f is a strict. Dec.fn. of S.

Remark 1: For a strictly increasing transmission function (f'(S) > 0 ∀ S > 0):

- DFE is glob.asymp. stable if $R_1 < 1$
- DFE becomes unstable if $R_1 > 1$
- An endemic equilibrium emerges and gains stability for $R_1 > 1$
- When $R_1 = 1$, the system is in transcritical bifurcation.

Remark 2: For a strictly decreasing transmission function (f'(S) < 0 ∀ S ∈ (0,1)):

- DFE exhibits:
  a. Local asymptotic stability when $R_0 < 1$
  b. Instability when $R_0 > 1$
- The EE is unstable whenever it exists
- The system demonstrates a backward bifurcation at $R_0 = 1$

From system (1),we have the no. of infect. individuals at time t using (1.1) is

$$\int_{I_0}^{I} \frac{dI}{I(f(1-I)-\phi(u)-\mu} = \int_0^t dt \tag{17}$$

(4)11

where I_0 is the initial value of I(t).

V.EXAMINATION OF FUZZY-BASED SYSTEM

Viral load-dependent dynamics are incorporated by modeling disease transmission $f(S,v)$ and treatment efficacy $\varphi(u,v)$ as fuzzy functions. Transmission occurs only if the viral load surpasses a minimum threshold $v_{\min}$, peaks at v_M, and saturates at $v_{\max}$, while treatment effectiveness varies with viral concentration. These relationships are mathematically represented through fuzzy membership functions (Eq. 5, Fig. 1), capturing the nonlinear increase in transmission risk with rising viral load and its impact on therapy.

Based on clinical estimations and prior literature, we assume:

- v_{min}= 0.2: Minimum viral load below which transmission and treatment are negligible.
- v_M = 0.6: Moderate viral load at which transmission and treatment start to become effective.
- v_{max} =1.0:Saturated viral load where transmission reaches its maximum and treatment is capped.

For the treatment response function $\phi(u,v)$, we introduce a capping factor (δ = 0.1), representing limitations in healthcare capacity or incomplete intervention. Hence, treatment effectiveness is bounded above by (1 - δ = 0.9).

The fuzzy classification of viral load ($\rho(v)$) is represented as a triangular membership function defined by the central value (v^C =0.6) and the spread (λ = 0.2). This allows the model to flexibly categorize viral intensity into linguistic levels such as low, moderate, and high, capturing the uncertain gradation of infection severity in the host population.These parameters are illustrated in Fig. 1 and form the basis for computing fuzzy transitions and intervention levels in the model simulations.

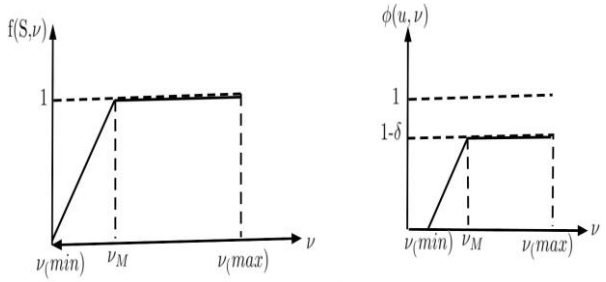

FIGURE 1. Membership Function of f (S, v) and $\phi(u,v)$.

(5)

$$f(S,v)=\begin{cases}0, if\, v<v_{\min},\\ \frac{f(S,v)-f(S,v_{\min})}{f(S,v_M)-f(S,v_{min})}, if\, v_{min}\le v\le_M,\\ 1, if\, v_M<v<v_{max}.\end{cases} \quad (18)$$

Treatment efficacy is highly dependent on disease severity, motivating the use of a fuzzy logic approach. When the viral load is below the threshold $v_{\min}$, no intervention is necessary. As the viral load increases within the range $v_{\min}\le v\le v_{\max}$, optimal treatment should ideally be administered. However, practical constraints such as cost limitations and medication shortages often hinder full implementation. To account for these real-world challenges, the treatment function is capped at $1-\delta$. This relationship is formally expressed through the membership function $\varphi(u)$ in Eq. (6).

$$\phi(u,v)=\begin{cases}0, \text{if } v<v_{min},\\ \frac{\phi(u,v)-\phi(u,v_{min})}{\phi(u,v_M)-\phi(u,v_{min})}(1-\delta), if\ v_{min}<v\le v_M,\\ 1-\delta, \text{if} v_M<v<v_{max}\ and\ \delta\ge 0\end{cases} \quad (19)$$

Building upon prior work, we have characterized both transmission dynamics and therapeutic interventions as fuzzy mappings dependent on viral burden (V), accounting for natural variations in infectious particle density across hosts. The viral quantity represents a qualitative linguistic parameter, whose categorical divisions are determined via clinical expertise. These graded classifications adopt triangular fuzzy set representations, mathematically specified in Eq. (7) and graphically illustrated in Fig. 2. The fuzzy classification of viral load ($\rho(v)$) is modeled using a triangular membership function that represents the degree of moderate viral intensity in the host population. This membership function is centered at the core viral load level (v^C=0.6), where the membership reaches its peak value of 1, indicating maximum classification as moderate.

The function linearly decreases on both sides, reaching zero at (v^C - λ = 0.4) and (v^C + λ = 0.8), where (λ = 0.2) is the spread parameter. This design captures the imprecise boundary between viral load categories, allowing the model to flexibly express transitions between low, moderate, and high levels of infection severity.

The shape and parameters of ($\rho(v)$) are illustrated in Fig.~2, and play a key role in modulating fuzzy rule-based transmission and intervention effects in the model.

$$\rho(v)=\begin{cases}0, \text{if } v<v^c-\lambda,\\ \frac{v-v^c+\lambda}{\lambda}, if\ v^c-\lambda\le v\le v^c,\\ -\frac{v-v^c-\lambda}{\lambda}, if\ v^c<v\le v^c+\lambda,\\ 1, if\ v>v^c+\lambda.\end{cases} \quad (20)$$

where,v^c and λ are the central and and dispersion values of every fuzzy set assumed by V.

VI. EXPLORATION OF A FUZZY SIS-BASED APPROACH TO MODELLING RIFT VALLEY FEVER VIRUS

If we consider f (S) = $f(S,v) and \phi(u) = \phi(u,v)$, then we can have the solution by solving

(8)

$$\int_{I_0}^{I} \frac{dI}{I(f(1-I,v)-\phi(u,v)-\mu} = \int_0^t dt \tag{21}$$

The system generates a set of solutions $I(v,t)$, representing time-dependent infected population density resulting from susceptible-infected interactions at a given viral concentration v. For any fixed t, the function $I(v,t)$ is a fuzzy number constrained within the interval [0,1] (see Eq.3). Applying defuzzification to $I(v,t)$ provides a deterministic estimate of infection prevalence at each time point.

VII.PROJECTED NUMBER OF RIFT VALLEY FEVER VIRUS CASES USING FUZZY LOGIC

Here, we ascertain the mathematical expectation of the count of infected subjects, expressed as $I(v,t)$.

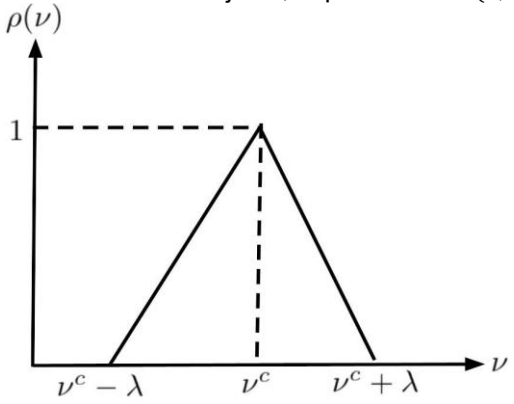

FIGURE 2. Membership Function of $\rho(v)$.

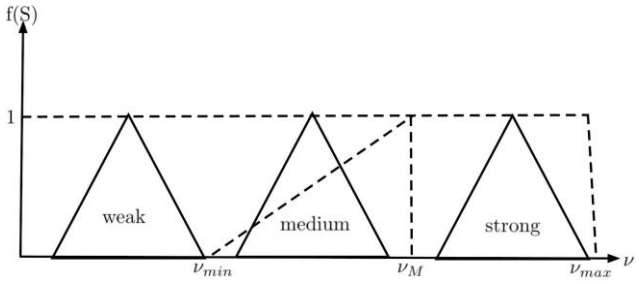

FIGURE3. Classification of linguistic variable V.

$$FEV[I] = \sup_{0\le\theta\le1}\inf[\theta, \zeta\{I \ge \theta\}] \tag{22}$$

The term $\zeta\{I \ge \theta\}$ quantifies the probability measure associated with the event where infection levels exceed threshold θ. The FEV[I] metric serves as an estimator for the standard expected value $E(I)$ of the infected population, offering computational efficiency by eliminating the need for integration.

Let $\Omega(\theta) = \zeta\{I \ge \theta\}$ for any $t > 0$. By definition, $\Omega(0) = 1$ (certainty of infection presence) and $\Omega(1) = 0$ (impossibility of complete infection). For intermediate thresholds $0 < \theta < 1$, the inequalities

$$f(S,v) \ge \Psi(\theta,t) \tag{23}$$

and

$$\phi(u,v) \ge \Psi(\theta,t) \tag{24}$$

emerge as necessary conditions when

$$I(v,t) \ge \theta.$$

$$\Omega(\theta) = \begin{cases} \zeta\{I(v,t) \ge \theta\}, \\ \zeta\{v: f(S,v), \phi(u,v) \ge \psi(\theta,t)\}, \\ 1, if \psi(\theta,t) \le 0, \\ \zeta[\chi, v_{max}], if 0 < \psi(\theta,t) \le 1, \\ 0, if \psi(\theta,t) > 1. \end{cases} \tag{25}$$

i.e.

$$\Omega(\theta) = \begin{cases} 1, 0 \le \theta \le I_0 \\ \zeta[\chi, v_{max}], I_0 < \theta \le I_1, \\ 0, I_1 < \theta \le 1. \end{cases} \tag{26}$$

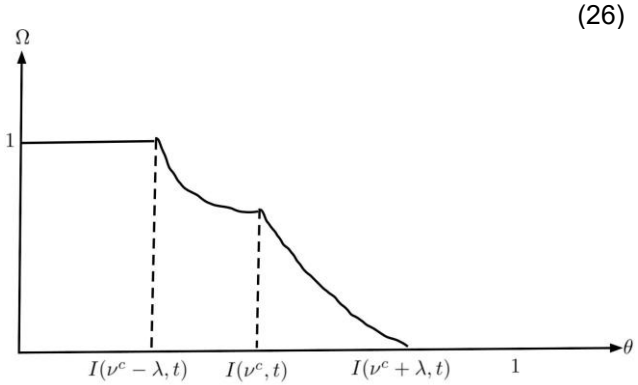

FIGURE 4. Graph of Ω.

We establish the parameter χ through the relation

$$\chi = v_{\min} + (v_M - v_{\min})\psi(\theta,t), \tag{26}$$

with I_1 being determined by optimizing the functions $f(S,v)$ and $\phi(u,v)$ at their respective maxima (unity and $1-\delta$) within the framework of equation (8). The parameter χ is bounded such that

$$v_{\min} < \chi \le v_M. \tag{27}$$

The fuzzy measure $\zeta(A)$ for any measurable subset $A \subset \mathbb{R}$ is formally expressed as:

$$\zeta(A) = \frac{1}{\lambda}\int_A \rho(\nu)d\nu, \tag{28}$$

where the normalized function $\rho(\nu)/\lambda$ constitutes a proper probability density, thereby rendering $\zeta(A)$ a well-defined probability measure on the real line.

For the estimation of $\mathrm{FEV}[I(\nu,t)]$, we employ a tripartite fuzzy classification system for the parameter ν:

- **Diminished range** (ν_l)
- **Intermediate range** (ν_m)
- **Elevated range** (ν_h)

These classifications are mathematically characterized through the boundary parameters $\nu_{\min}, \nu_M$, and $\nu_{\max}$, with their graphical representation illustrated in Figure 3. The fuzzy sets corresponding to these classifications exhibit standard membership function properties while maintaining computational tractability for epidemiological modeling purposes.

Subthreshold Case (ν_l): When viral load remains below critical levels $(\nu^c + \lambda < \nu_{\min})$, containment measures render $\zeta[\chi, \nu_{\max}] = 0$. The binary $\Omega(\theta)$ transitions sharply at $\theta = I_0$, yielding

$$\mathrm{FEV}[I(\nu,t)] = I_0, \tag{29}$$

confirming disease suppression.

Moderate Case (ν_m): For intermediate viral loads $(\nu^c - \lambda > \nu_{\min}, \nu^c + \lambda < \nu_m)$, $\Omega(\theta)$ displays smooth quadratic decay, ensuring a unique equilibrium

$$\mathrm{FEV}[I(\nu,t)] = I(\nu^c, t) \tag{30}$$

at the endemic balance point $I(\nu^c, t) = 0.5$.

Suprathreshold Case (ν_h): At high concentrations $(\nu^c - \lambda \geq \nu_m, \nu^c + \lambda \leq \nu_{\max})$, $\zeta[\chi, \nu_{\max}]$ saturates, producing a step-function $\Omega(\theta)$. $\mathrm{FEV}[I(\nu,t)]$ converges to the classical solution under maximal transmission $(f = 1)$ and reduced treatment efficacy $(\phi = 1 - \delta)$.

The medium case particularly demonstrates equilibrium where FEV matches the infection function's fixed point, representing stable endemic conditions.

$$FEV[I(\nu,t)] < I(\nu^c,t), if I(\nu^c,t) > \frac{1}{2} \tag{31}$$

$$FEV[I(\nu,t)] > I(\nu^c,t), if I(\nu^c,t) > \frac{1}{2} \tag{32}$$

The $\mathrm{FEV}[I(\nu,t)]$ is derivable for arbitrary fuzzy measures ξ. Specifically, if ξ represents possibility, we obtain

$$\mathrm{FEV}[I(\nu,t)] = \sup[\xi(\nu) \wedge I(\nu,t)]. \tag{33}$$

$$\xi(X) = \sup\rho(\nu), \nu \in X, X \subset R$$

So,we have,

$$\Omega(\theta) = \begin{cases} 1, if 0 \leq \theta \leq I_0, \\ \sup\limits_{\nu\in[\chi,\nu_{max}]} \rho(\nu), if I_0 < \theta \leq I_1, \\ 0, if I_1 < \theta \leq 1. \end{cases} \tag{34}$$

and $FEV[I(\nu,t)]$ is the fixed point of $\Omega(\theta)$.

The expectation $E[I(\nu,t)]$ for the no. of infected individuals is now computed for the three key cases: $\nu_{\min}, \nu_M$, and $\nu_{\max}$, according to the previous definitions.

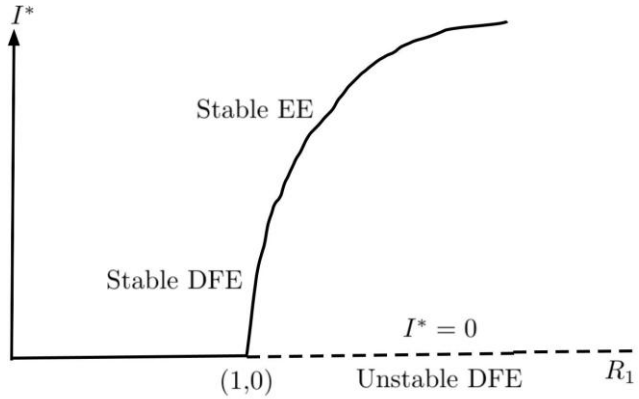

FIGURE 5. Curve of transcritical bifurcation.

VIII.CONVENTIONAL ASSESSMENT OF RIFT VALLEY FEVER VIRUS INFECTION COUNT

The expected no. of infected individuals at time t under random parameter v is

$$E[I(\nu,t)] = \int_{-\infty}^{+\infty} I(\nu,t)\frac{\rho(\nu)}{\lambda}d\nu = \frac{1}{\lambda}\int_{\nu^c-\lambda}^{\nu^c+\lambda} I(\nu,t)\rho(\nu)d\nu. \tag{35}$$

In the low-virus scenario (ν_l), where $\nu^c + \lambda < \nu_{\min}$, the disease transmission function $f(S,\nu)$ is entirely suppressed for all infected individuals, resulting in an expectation

$$E[I(\nu,t)] = I_0. \tag{36}$$

In the intermediate-virus case (ν_m), where $\nu^c - \lambda > \nu_{\min}$ and $\nu^c + \lambda < \nu_M$, $f(S,\nu)$ exhibits variability, and $E[I(\nu,t)]$ is derived through integration, contingent upon the knowledge of all relevant parameters.

Conversely, in the high-virus condition (ν_h), where $\nu^c - \lambda \geq \nu_M$ and $\nu^c + \lambda \leq \nu_{\max}$, the transmission function $f(S,\nu)$ attains its upper bound of 1, signifying maximal contagion among infected individuals.

Hence, we have

$$E[I(v,t)] = \frac{1}{\lambda}\int_{v^c-\lambda}^{v^c-\lambda} \rho(v)I(v,t)dv = I_1 \tag{37}$$

IX.INFLUENCE OF AN EXPANDING TRANSMISSION FUNCTION ON RIFT VALLEY FEVER EQUILIBRIA AND BIFURCATION

The basic reprodn.no.R_1 works as a fundamental epidemic threshold parameter. It assesses the expected no. of secondary infections created by an infected individual in a suspected population. Epidemic expansion occurs when $R_1 > 1$, while $R_1 < 1$ signifies disease extinction.
For this system, the reproduction number (RN) is given by

$$R_1 = \frac{f(1)}{\varphi(u)+\mu} \tag{38}$$

which governs a transcritical bifurcation at $R_1 = 1$, where the DFE loses stability, giving rise to an endemic state. Interestingly, the EE remains stable even below this threshold when

$$I^* > -\frac{\mu}{f'(S^*)}. \tag{39}$$

Viral load dependence introduces a critical concentration v^*, satisfying

$$f(1,v^*) = \varphi(u,v^*) + \mu, \tag{40}$$

which triggers the bifurcation within the interval $[v_{\min}, v_M]$, as illustrated in Fig. 5. The bifurcation structure illustrated in Fig.~5 depicts a transcritical bifurcation, which is a typical feature of classical epidemic models. The figure plots the infected population I* against the basic reproduction number R_1, providing insight into the stability of disease equilibria as transmission conditions change.

At the critical threshold $R_1 = 1$, a stability exchange occurs between the disease-free equilibrium (DFE) and the endemic equilibrium (EE):

When $R_1 < 1$, I*=0 the DFE at is stable, meaning that the disease cannot invade the population and will eventually die out.

As R_1 crosses 1 and becomes greater than 1, the DFE becomes unstable, and a stable endemic equilibrium emerges where I*>0, signifying persistent infection in the population.

The two equilibria intersect at the bifurcation point (R_1, I*) = (1, 0), where the transition from the disease-free to the endemic state occurs.

This transcritical bifurcation indicates that controlling the reproduction number R_1 below 1 is both necessary and sufficient for disease eradication. Unlike backward bifurcation, no multiple stable endemic states exist when R_1<1, making intervention strategies more straightforward in this case.The behavior illustrated in Fig. 5 is representative of models with **linear or monotonic incidence rates** and without saturation or fuzzy uncertainty in key parameters. It serves as a baseline case in comparing more complex bifurcation structures arising in fuzzy or stochastic systems.
This virus-driven model necessitates the use of a fuzzy RN to accurately describe the uncertainties associated with transmission dynamics.

$$R_1^f = \frac{1}{1-\delta+\mu} FEV[(1-\delta+\mu)R_1(v)] \tag{41}$$

where $R_1(v) = \frac{f(1,v)}{\phi(u,v)+\mu}$. It is found that $R_1(v)$ may be greater than 1, but $[(1-\delta+\mu)R_1(v)]$ is always a +ive fract. with highest value 1. To get FEV$[(1-\delta+\mu)R_1(v)]$, we use the likelihood assessment $\psi(X)$ as

$$\psi(X) = \sup\rho(v), v \in X \subset R \tag{42}$$

The *group infectivity index* is defined by the maximal individual infectivity within the group, representing a worst-case transmission scenario.We compute the fuzzy basic reproduction number R^f_1 by incorporating viral load levels (*low, medium, high*) through their associated membership functions ρ(v). The analysis considers the following cases:

(a) low if $v^c + \lambda < v_{min}$
(b) medium if $v^c - \lambda > v_{min}$ and $v^c + \lambda \le v_M$
(c) high if $v^c - \lambda > v_M$.

In the scenario where viral load is minimal (Case a), it is self-evident that the fuzzy basic reproduction number satisfies $R_1^f < 1$. To ascertain R_1^f for the subsequent cases (b) and (c), we leverage the strictly monotonous nature of $R_1(v)$, yielding the relation

$$\Omega(\theta) = \phi[v, v_{\max}] = \sup\rho(v), \quad v' \le v \le v_{\max},$$

where v' is the soln. to the eqn.

$$(1-\delta+\mu)\frac{f(1,v)}{\phi(u,v)+\mu} = \theta. \tag{43}$$

Through analytical derivation in Case (b), the function $\Omega(\theta)$ assumes a segmented form, substantiating that the fuzzy expected value

$$FEV[(1-\delta+\mu)\frac{f(1,v)}{\phi(u,v)+\mu}] \tag{44}$$

coincides with the fixed point of Ω, thereby satisfying the inequality

$$R_1(\nu^c) < R_1^f < R_1(\nu^c + \lambda). \tag{45}$$

Extending this result to Case (c), we deduce the bound

$$\frac{1}{\phi(u,\nu^c)} < R_1^f < \frac{1}{\phi(u,\nu^c+\lambda)+\mu}, \tag{46}$$

signifying that the disease will establish itself if

$$R_1^f > \frac{1}{\phi(u,\nu^c)} > 1. \tag{47}$$

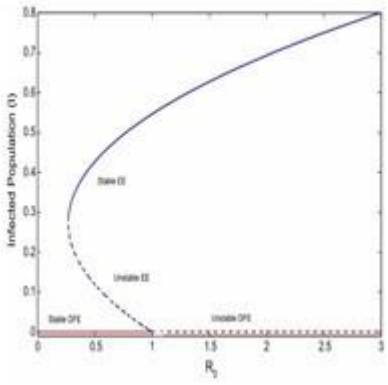

FIGURE 6. Curve of Backward Bifurcation.

X.FUZZY EPIDEMIC INTERVENTIONS FOR RIFT VALLEY FEVER WITH AN INTENSIFYING TRANSMISSION FUNCTION

Disease dynamics in this framework are significantly influenced by viral load ν, transmission efficiency $f(S)$, and treatment efficacy $\varphi(u)$. The fuzzy formulation of system (0.1) generates a continuum of viral-dependent models, which can be effectively approximated by a single characteristic system at an optimal viral concentration ν^*.

A. Viral Load Scenarios

1) Subthreshold Viral Levels ($\nu < \nu_{min}$)

- The RN: $R_1(\nu) = 0\ (< 1)$
- Disease elimination occurs inevitably

2) Moderate Viral Loads ($\nu_{min} \le \nu \le \nu_M$)

Three distinct epidemiological outcomes emerge:

1. $\nu^* < \nu$: $R_1(\nu) < 1$ → Disease-free state
2. $\nu^* = \nu$: $R_1(\nu) = 1$ → Transcritical bifurcation occurs
3. $\nu^* > \nu$: $R_1(\nu) > 1$ → Endemic establishment

3) High Viral Concentrations ($\nu \in [\nu_{min}, \nu_M]$)

Disease spread is governed by the treatment parameter δ:

1. $\delta < \mu$: $R_1(\nu^*) < 1$ → Pathogen clearance
2. $\delta > \mu$: $R_1(\nu^*) > 1$ → Epidemic propagation
3. $\delta = \mu$: Bifurcation induces oscillatory dynamics near the DFE

XI.BASIC REPRODUCTION NUMBER AND NONLINEAR DYNAMICS IN RIFT VALLEY FEVER WITH A DECLINING DISEASE TRANSMISSION FUNCTION

The epidemic threshold is determined by:

$$R_0 = \frac{f(S^{**})}{\varphi(\nu)+\mu} \tag{48}$$

with stability reversal occurring at $R_0 = 1$. At this critical point, the DFE transitions from stability to instability, indicating a backward bifurcation (Fig. 6). The condition:

$$f(S,\nu) = \varphi(u,\nu) + \mu \tag{49}$$

identifies a specific viral concentration ν^{**} (where $\nu_{\min} < \nu^{**} < \nu_M$) that initiates this bifurcation.
The bifurcation curve shown in Fig.~6 illustrates the dynamics of the infected population I as a function of the basic reproduction number R_0, highlighting the presence of backward bifurcation in the system. Unlike classical models where the disease-free equilibrium (DFE) is globally stable for (R_0 < 1), this model exhibits a critical threshold below 1, at which multiple equilibria coexist.

Specifically, for values of R_0 just below 1, two endemic equilibria (EE)—one stable and one unstable—emerge alongside a stable DFE. This implies that disease eradication is not guaranteed even if $R_0 < 1$, due to the existence of a stable endemic equilibrium. The turning point on the bifurcation curve denotes the critical value of R_0 where the bifurcation occurs.

This behavior is characteristic of models with imperfect treatment, nonlinear incidence, or fuzzy parameter dependencies, such as those arising in viral load-dependent transmission. The presence of backward bifurcation in this model underscores the importance of maintaining intervention efforts even when R_0 appears to fall below unity, as infection can persist due to residual endemic stability.

These features are vital for understanding control thresholds and treatment saturation effects, particularly in fuzzy or uncertain environments modeled using fuzzy logic or stochastic frameworks.

A.Fuzzy Reproduction Number

The fuzzy RN is formulated as:

$$R_0^f = \frac{1}{1-\delta+\mu}\,\mathrm{FEV}[(1-\delta+\mu)R_0(\nu)], \tag{49}$$

where:

$$R_0(\nu) = \frac{f(S^{**},\nu)}{\varphi(u,\nu)+\mu}. \tag{50}$$

Notably, $(1-\delta+\mu)R_0(\nu)$ remains bounded within $(0,1]$.

B. Viral Load Classification & System Behavior

1) Low Viral Load ($\boldsymbol{\nu_c + \lambda < \nu_{min}}$)

Ensures $R_0^f < 1$, preventing disease persistence.

2) Medium Viral Load ($\boldsymbol{\nu_c - \lambda > \nu_{min}}$ and $\boldsymbol{\nu_c + \lambda \le \nu_M}$)

The fuzzy expectation $\Omega(\theta)$ follows a piecewise structure:

$$\Omega(\theta) = \begin{cases} 1, & \theta \le (1-\delta+\mu)R_0(\nu_c), \\ \rho(\nu''), & \text{forintermediate}\theta, \\ 0, & \theta > (1-\delta+\mu)R_0(\nu_c+\lambda). \end{cases} \tag{51}$$

Here, $R_0(\nu_c) < R_0^f < R_0(\nu_c+\lambda)$.

3) High Viral Load ($\boldsymbol{\nu_c - \lambda > \nu_M}$)

Disease invasion requires:

$$R_0^f > \frac{1}{\varphi(u,\nu_c)} > 1, \tag{52}$$

highlighting the critical role of treatment efficacy δ in controlling outbreaks.

XII.FUZZY EPIDEMIC-BASED CONTROL STRATEGIES FOR RIFT VALLEY FEVER UNDER A DECLINING DISEASE TRANSMISSION FUNCTION RELATIVE TO THE SUSCEPTIBLE GROUP

The disease control dynamics in this system depend critically on three factors: viral load (ν), disease transmission function $f(S)$, and treatment efficacy $\varphi(u)$. The fuzzy formulation generates a continuum of systems parameterized by ν, which can be reduced to an equivalent single system at an optimal viral concentration ν^{**}.

Viral Load Scenarios

1. *Subthreshold Viral Levels ($\boldsymbol{\nu^{**} < \nu_{min}}$)*

The basic reproduction number becomes negligible ($R_1 < 1$), leading to disease elimination.

2. *Moderate Viral Loads ($\boldsymbol{\nu_{min} \le \nu^{**} \le \nu_M}$)*

Three distinct epidemiological outcomes emerge:

a. If $\nu^{**} < \nu^{**}$, the system remains disease-free ($R_1 < 1$).

b. At the critical threshold $\nu^{**} = \nu^{**}$, a transcritical bifurcation occurs ($R_1 = 1$).

c. For $\nu^{**} > \nu^{**}$, the disease becomes endemic ($R_1 > 1$).

3. *High Viral Concentrations ($\boldsymbol{\nu^{**} \in [\nu_{min}, \nu_M]}$)*

The epidemic outcome depends crucially on the treatment parameter δ:

- If $\delta < \mu$, the disease dies out ($R_1 < 1$).
- If $\delta > \mu$, the infection spreads ($R_1 > 1$).
- At the exact balance point $\delta = \mu$, the system exhibits oscillatory behavior around the DFE.

XIII.SIMULATED COMPUTATION

Linear functional forms are adopted to characterize disease transmission and therapeutic intervention, expressed as:

$$f(S) = \beta S \tag{53}$$

where β represents the transmission rate, and

$$\varphi(u) = m + bu \tag{54}$$

incorporating baseline recovery m and treatment coefficient b.The system of DE governing the susceptible and infected populations is given by:

$$\frac{dS}{dt} = \mu - \beta SI + (m+bu)I - \mu S \tag{55}$$

$$\frac{dI}{dt} = \beta SI - (m+bu+\mu)I \tag{56}$$

$\beta = 0.38, \mu = 0.001, u = 0.5, b = 0.003, m = 0.01$ numerical analysis reveals asymptotic convergence to the endemic equilibrium (Fig. 7). Remarkably, this stability emerges even with a subthreshold reproduction number: R_1 = 0.9971 and persists under strictly increasing transmission dynamics, underscoring the system's capacity to sustain endemicity below conventional epidemic thresholds.

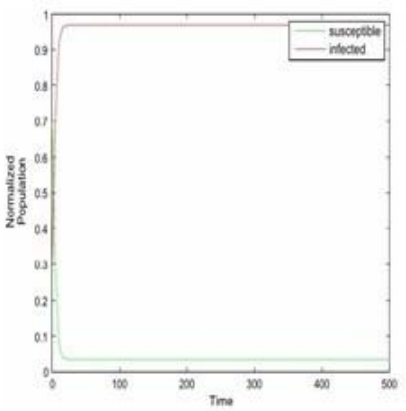

FIGURE 7. System is asymptoticaly stable at endemic equilibrium.

XIV.CONCLUSION

This study investigates an SIS (Susceptible-Infected-Susceptible) contagion model in which the infection propagation rate and therapeutic intervention efficacy are modeled as generalized functions of the vulnerable subpopulation (S) and the treatment parameter (u), respectively. The analysis begins by evaluating the dynamic characteristics of the traditional (non-fuzzy) system, focusing on cases where the medical response function exhibits either a strictly escalating or diminishing relationship with S. Notably, a stable endemic state can emerge even when the basic reproduction threshold (R_0) is below one, particularly under a declining contagion rate. The system's equilibrium behavior is analyzed in relation to R_0 for both upward- and downward-sloping treatment functions. The study then advances to a fuzzy-logic-based extension, where both transmission dynamics and healthcare measures are expressed as functions of the prevailing pathogen load. Affiliation distributions for both pathogen dissemination and clinical intervention effectiveness are precisely characterized. The probabilistic projection of affected cases is established and stratified according to pathogen quantity (minimal, intermediate, substantial). Furthermore, a probabilistic proliferation index (a measure of the likelihood that an infection will spread within a population under uncertain conditions) is constructed and evaluated. A pivotal microorganism density benchmark (a critical threshold of microorganism concentration indicating when infection risk significantly rises) is discovered where the adapted probabilistic SIS framework demonstrates either transitional or reverse divergence, contingent on whether the infection dispersal escalates or diminishes relative to the vulnerable cohort (S). In forthcoming scholarly inquiry, we propose integrating supplementary parameters into the paradigm to augment its ecological verisimilitude. Established computational schemata, particularly the Receptive-Contagious-

Receptive (RCR) disease propagation construct, are ubiquitously implemented to examine the diffusion of transmissible pathologies, including Rift Valley Fever (RVF). These theoretical representations enable simulation of outbreak progression patterns and optimize containment methodologies.

ACKNOWLEDGEMENT

We thank the reviewers and editor of the journal for their guidance in improving the quality of our article.

FUNDING STATEMENT

This work is supported by the Alagappa University Research Fund (AURF) Seed Money 2024 [grant sanctioned vide Letter No. AU/SO(P&D)/AURF Seed Money/2024 Alagappa University, Karaikudi, Tamil Nadu, India, Date 11th December 2024]

AUTHOR CONTRIBUTION

Meyyappan Sangavi: Conceptualization, Methodology, Data Curation, Mathematical Modeling, Numerical Simulations, Writing – Original Draft Preparation;

M. Vidhya Lakshmi: Validation, Visualization, Writing – Review & Editing, Investigation;

Murugappan Mullai: Supervision, Project Administration, Methodology Refinement, Writing – Review & Editing;

Grienggrai Rajchakit: Theoretical Analysis, Stability and Bifurcation Analysis, Writing – Review & Editing;

Govindan Vetrivel: Supervision, Funding Acquisition, Critical Review, Writing – Review & Editing.

CONFLICT OF INTEREST

The authors declare that there is no conflict of interest regarding the publication of this paper.

ETHICS STATEMENT

This research did not involve human participants, animal subjects, or sensitive personal data, and therefore did not require ethical approval.

REFERENCES

[1] S. Adak and S. Jana, "A study on stegomyia indices in dengue control: a fuzzy approach," *Soft Computing*, vol. 25, no. 1, pp. 699–709, 2021. DOI: https://doi.org/10.1007/s00500-020-05179-x

[2] M.S. Arif, A. Ahmad and M. Khan, "Construction of a computational scheme for the fuzzy HIV/AIDS epidemic model with a nonlinear saturated incidence rate," *Computer Modeling in Engineering & Sciences*, vol. 138, no. 2, pp. 1405–1425, 2024. DOI: https://doi.org/10.32604/cmes.2023.028946

[3] M.S. Arif, A. Ahmad and M. Khan, "A hybrid SIR-fuzzy model for epidemic dynamics: A numerical study," *Computer Modeling in Engineering & Sciences*, vol. 139, no. 3, pp. 3417–3434, 2024. DOI: https://doi.org/10.32604/cmes.2024.046944

[4] J. Arino, K.L. Cooke, P. Driessche and J. Valesco-Hernandez, "An epidemiology model that includes a leaky

vaccine with a general waning function," *Journal of Differential Equations*, vol. 4, no. 2, pp. 479–495, 2004. DOI: https://doi.org/10.3934/dcdsb.2004.4.479

[5] R. Azerigyik and S.F. Sallam, "The temperature-associated effects of Rift Valley Fever virus infections in mosquitoes and climate-driven epidemics: A review," *Viruses*, vol. 17, no. 2, p. 217, 2025. DOI: https://doi.org/10.3390/v17020217

[6] N.S. Barlow and S.J. Weinstein, "Accurate closed-form solution of the SIR epidemic model," *Physica D: Nonlinear Phenomena*, vol. 408, p. 132540, 2020. DOI: https://doi.org/10.1016/j.physd.2020.132540

[7] F. Brauer, "Backward bifurcation in simple vaccination treatment models," *Journal of Biological Dynamics*, vol. 5, no. 5, pp. 410–418, 2011. DOI: https://doi.org/10.1080/17513758.2010.510584

[8] V. Capasso and G. Serio, "A generalization of the Kermack-Mackendrick deterministic epidemic model," *Mathematical Biosciences*, vol. 42, no. 1–2, pp. 43–61, 1978. DOI: https://doi.org/10.1016/0025-5564(78)90006-8

[9] X. Cao and Z. Jin, "Epidemic threshold and ergodicity of an SIS model in switched networks," *Journal of Mathematical Analysis and Applications*, vol. 479, no. 1, pp. 1182–1194, 2019. DOI: https://doi.org/10.1016/j.jmaa.2019.06.074

[10] J.C. Eckalbar and W.L. Eckalbar, "Dynamics of an epidemic model with quadratic treatment," *Nonlinear Analysis: Real World Applications*, vol. 12, no. 1, pp. 320–332, 2011. DOI: https://doi.org/10.1016/j.nonrwa.2010.06.018

[11] R.E. Morrison and A. Cunha Jr, "Embedded model discrepancy: A case study of Zika modeling," *arXiv preprint*, 2020. DOI: https://doi.org/10.48550/arXiv.2004.06220

[12] A.B. Gumel and S.M. Moghadas, "A qualitative study of a vaccination model with nonlinear incidence," *Applied Mathematics and Computation*, vol. 143, no. 2–3, pp. 409–419, 2003. DOI: https://doi.org/10.1016/S0096-3003(02)00372-7

[13] H.W. Hethcote, "The mathematics of infectious diseases," *SIAM Review*, vol. 42, no. 4, pp. 599–653, 2000. DOI: https://doi.org/10.1137/S0036144500371907

[14] Z. Hu, W. Ma and S. Ruan, "Analysis of SIR epidemic models with nonlinear incidence rate and treatment," *Mathematical Biosciences*, vol. 238, no. 1, pp. 12–20, 2012. DOI: https://doi.org/10.1016/j.mbs.2012.03.010

[15] S. Jana, P. Haldar and T.K. Kar, "Optimal control and stability analysis of an epidemic model with population dispersal," *Chaos, Solitons & Fractals*, vol. 83, pp. 67–81, 2016. DOI: https://doi.org/10.1016/j.chaos.2015.11.018

[16] T.K. Kar and S. Jana, "Application of three controls optimally in vector borne disease—A mathematical study," *Communications in Nonlinear Science and Numerical Simulation*, vol. 18, no. 10, pp. 2868–2884, 2013. DOI: https://doi.org/10.1016/j.cnsns.2013.01.022

[17] E. Purssell, D. Gould and J. Chudleigh, "Impact of isolation on hospitalised patients who are infectious: systematic review with meta-analysis," *BMJ Open*, vol. 10, no. 2, pp. e030371, 2020. DOI: https://doi.org/10.1136/bmjopen-2019-030371

[18] T.K. Kar and S. Jana, "A theoretical study on mathematical modelling of an infectious disease with application of optimal control," *BioSystems*, vol. 111, no. 1, pp. 37–50, 2013. DOI: https://doi.org/10.1016/j.biosystems.2012.10.003

[19] T.K. Kar and P.K. Mondal, "Global dynamics of a tuberculosis epidemic model and the influence of backward bifurcation," *Journal of Mathematical Modelling and Algorithms*, vol. 11, no. 4, pp. 433–459, 2012. DOI: https://doi.org/10.1007/s10852-012-9210-8

[20] P. Monisha, and S. S. Devi, " Analyzing Dynamical Behavior of Tuberculosis Transmission," *Contemporary Mathematics*, vol. 4, no. 4, pp. 1331–1345, 2023. DOI: https://doi.org/10.37256/cm.4420232621

[21] A. Kumar and J. Susan, "Epidemic modeling using hybrid of time-varying SIRD, particle swarm optimization, and deep learning," *arXiv preprint*, 2024. DOI: https://arxiv.org/abs/2401.18047

[22] H. Laarabi, A. Abta and K. Hattaf, "Optimal control of a delayed SIRS epidemic model with vaccination and treatment," *Acta Biotheoretica*, vol. 63, no. 2, pp. 87–97, 2015. DOI: https://doi.org/10.1007/s10441-015-9244-1

[23] H. Rafiei, A. Salehi, F. Baghbani, P. Parsa and M.R. Akbarzadeh-T, "Interval type-2 fuzzy control and stochastic modeling of COVID-19 spread based on vaccination and social distancing rates," *Computer Methods and Programs in Biomedicine*, vol. 232, p. 107443, 2023. DOI: https://doi.org/10.1016/j.cmpb.2023.107443

[24] O.D. Makinde, "Adomian decomposition approach to a SIR epidemic model with constant vaccination strategy," *Applied Mathematics and Computation*, vol. 184, no. 2, pp. 842–848, 2007. DOI: https://doi.org/10.1016/j.amc.2006.06.074

[25] E. Massad, N. R. S. Ortega, L.C.D. Barros and C.S. Struchiner, "Fuzzy Logic in Action: Application of Epidemiology and Beyond", 1st ed., *Springer*, 2008. DOI: https://doi.org/10.1007/978-3-540-69094-8

[26] B.K. Mishra and M.K. Pandey, "Fuzzy epidemic model for the transmission of worms in a computer network," *Nonlinear Analysis: Real World Applications*, vol. 11, no. 5, pp. 4335–4341, 2010. DOI: https://doi.org/10.1016/j.nonrwa.2010.05.018

[27] P.K. Mondal, S. Jana, P. Haldar and T.K. Kar, "Dynamical behavior of an epidemic model in a fuzzy transmission," *International Journal of Uncertainty, Fuzziness and Knowledge-Based Systems*, vol. 23, no. 5, pp. 651–665, 2015. DOI: https://doi.org/10.1142/S0218488515500282

[28] J.D. Murray, "Mathematical Biology," 3rd ed., *Springer*, 2002. DOI: https://doi.org/10.1007/b98868

[29] G. Niu and Y. Yan, "Stability and bifurcation analysis of an SIR model with saturated incidence and treatment," *Nonlinear Analysis: Real World Applications*, vol. 20, pp. 1–15, 2014. DOI: https://arxiv.org/abs/1501.06179

[30] Q. Cao, Y. Liu and W. Yang, "Global dynamics of a diffusive SIR epidemic model with saturated incidence rate and discontinuous treatments," *International Journal of Dynamics and Control*, vol. 10, pp. 1770–1777, 2022. DOI: https://doi.org/10.1007/s40435-022-00935-3

[31] M. Abdy, S. Side, S. Annas, W. Nur and W. Sanusi, "An SIR epidemic model for COVID-19 spread with fuzzy parameters: the case of Indonesia," *Advances in Difference Equations*, vol. 2021, p. 105, 2021. DOI: https://doi.org/10.1186/s13662-021-03263-6

[32] S. He and Y. Peng, "Application of a time-delay SIR model with vaccination in COVID-19 prediction and its optimal control strategy," *Nonlinear Dynamics*, vol. 111, pp. 10677–10692, 2023. DOI: https://doi.org/10.1007/s11071-023-08308-x

[33] S.C. Mpeshe, "Fuzzy SEIR epidemic model of Amoebiasis infection in humans," *Advances in Fuzzy Systems*, vol. 2022, p. 5292830, 2022. DOI: https://doi.org/10.1155/2022/5292830

[34] A. Subramanian, R. Sharma and M. Patel, "Fuzzy fractional Caputo derivative of susceptible-infectious-removed epidemic model for childhood diseases," *Mathematics*, vol. 12, no. 3, p. 466, 2024. DOI: https://doi.org/10.3390/math12030466

[35] L.A. Zadeh, "Fuzzy sets as a basis for a theory of possibility," *Fuzzy Sets and Systems*, vol. 1, no. 1, pp. 3–28, 1978. DOI: https://doi.org/10.1016/0165-0114(78)90029-5

[36] S. Jana, S. Nandi and T.K. Kar, "Complex dynamics of an SIR epidemic model with saturated incidence rate and treatment," *Acta Biotheoretica*, vol. 64, pp. 65–84, 2016. DOI: https://doi.org/10.1007/s10441-015-9273-9

[37] K. Goel, A. Kumar and Nilam, "Nonlinear dynamics of a time-delayed epidemic model with two explicit aware classes, saturated incidences, and treatment," *Nonlinear Dynamics*, vol. 101, pp. 1693–1715, 2020. DOI: https://doi.org/10.1007/s11071-020-05762-9

[38] V. Padmapriya and M. Kaliyappan, "A fuzzy fractional mathematical model of COVID-19 epidemic," *Journal of Intelligent & Fuzzy Systems*, pp. 1–23, 2022. DOI: https://doi.org/10.3233/JIFS-211173

[39] V. Padmapriya and M. Kaliyappan, "Fuzzy fractional mathematical model of COVID-19 epidemic," *Journal of Intelligent & Fuzzy Systems*, vol. 42, no. 4, pp. 3299-3321, 2022. DOI: https://doi.org/10.3233/jifs-211173

[40] M. Helikumi and P.O. Lolika, "Global dynamics of fractional-order model for malaria disease transmission," *Asian Research Journal of Mathematics*, vol. 18, no. 9, pp. 82–110, 2022.
DOI: https://doi.org/10.9734/ARJOM/2022/v18i930409

[41] G. Vijayalakshmi, R. Vikram, A. Akgül and M.K. Hassani, "Fuzzy mathematical modelling on diabetic and non-diabetic cases after vaccination," *Results in Engineering*, vol. 27, pp. 105888, 2025.
DOI: https://doi.org/10.1016/j.rineng.2025.105888

[42] F. Brauer and C. Castillo-Chavez, “Mathematical Models in Population Biology and Epidemiology,” 2nd ed., *Springer*, 2012.
DOI: https://doi.org/10.1007/978-1-4614-1686-9

[43] H. Sakkas, P. Bozidis, A. Franks and C. Papadopoulou, "Oropouche fever: A review," *Viruses*, vol. 10, no. 4, p. 175, 2018.
DOI: https://doi.org/10.3390/v10040175

[44] S. Hussain, N. Iqbal, E.N. Madi, M. Bakouri, I. Khan and W.S. Koh, "On the stochastic modeling and forecasting of the SVIR epidemic dynamic model under environmental white noise," *AIMS Mathematics*, vol. 10, no. 2, pp. 3983–3999, 2025.
DOI: https://doi.org/10.3934/math.2025186